Scilight

Bioelectrochemistry and Biosensors

https://www.sciltp.com/journals/bebs

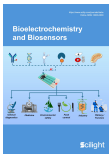

Review

Electrochemical Localized Surface Plasmon Resonance: Review and Theoretical Consideration

Andrii Lopatynskyi [1,2], Petro Demydov [1], Vitalii Lytvyn [1], Mariia Khutko [1] and Volodymyr Chegel [1,2,3,*]

[1] V. Lashkaryov Institute of Semiconductor Physics NAS of Ukraine, 41, Prospect Nauky, 03028 Kyiv, Ukraine
[2] Educational and Scientific Institute of High Technologies, Taras Shevchenko National University of Kyiv, 64/13, Volodymyrska Str., 01601 Kyiv, Ukraine
[3] UCCS Biofrontiers Center, University of Colorado Colorado Springs, 1420 Austin Bluffs Parkway, Colorado Springs, CO 80918-3733, USA
* Correspondence: chegelvi@outlook.com

How To Cite: Lopatynskyi, A.; Demydov, P.; Lytvyn, L.; et al. Electrochemical Localized Surface Plasmon Resonance: Review and Theoretical Consideration. *Bioelectrochemistry and Biosensors* **2025**, *1*(1), 2.

Received: 1 October 2025
Revised: 3 November 2025
Accepted: 17 November 2025
Published: 27 November 2025

Abstract: An overview of the current state of research in the field of electrochemical localized surface plasmon resonance (electrochemical LSPR, ELSPR) is presented. The model based on the Mie scattering theory for spherical particles and the Stern electrical double layer theory were exploited for computer modelling of the influence of parameters of the "gold nanoparticle-electrolyte" system on the extinction spectra and the LSPR position of a gold nanoparticle upon applying an electric potential difference between the nanoparticle and the surrounding electrolyte in the range of −0.3 to +0.6 V. It was shown that the extinction spectra undergo non-linear and mostly non-monotonic shifts in intensity and wavelength depending on the magnitude of the applied potential at all nanoparticle sizes in the radius range of 5–80 nm. It was established that the resulting shift in the LSPR position with changes in potential difference in the range of −0.3 to +0.6 V depends on the size of the nanoparticle, the refractive index of the electrolyte, the concentration of the electrolyte, the potential of zero charge of the nanoparticle in the electrolyte, and the charge of the ion in the electrolyte, and can reach amplitude values from 0.3 nm to 5.6 nm.

Keywords: localized surface plasmon resonance; electrochemistry; gold nanoparticles; light extinction; electrical double layer; electric potential

1. Introduction

The features of the electrochemical localized surface plasmon resonance (ELSPR) method, which combines simultaneous measurements using electrochemical and optical techniques in systems based on plasmonic nanostructures, have recently been researched more extensively. This is related to the prospects of applying the ELSPR method for sensing, photovoltaics, chemical catalysis, light modulation on a nanoscale, creation of metamaterials, and electro-optical converters. The advantages of this method include the ability to simultaneously obtain multidimensional information about the optical and electrochemical properties of the studied systems, adjust the spectral characteristics of the LSPR and related sensor response by applying an electrical signal, and convert local electric fields into an optical signal with high spatiotemporal resolution.

The foundations of the ELSPR methodology were introduced in the 1980s in several studies on the influence of applied electric potential on the dispersion of surface plasmon-polaritons in thin films of silver and gold under contact with an electrolyte [1,2]. It was established that the energy of plasmonic excitations depends on the magnitude of the applied potential [1] and the type of electrolyte [2]. Later, it was discovered that the plasmonic response to the application of an alternating potential allows for the study of both Faradaic and non-Faradaic

processes at the “metal-electrolyte” interface, and also contains specific features associated with surface effects that cannot be investigated only through electrochemical measurements [3]. In the late 1990s, the results of the first spectroelectrochemical studies of silver and gold nanoparticles were published. In particular, it was shown that the spectral position of the LSPR of colloidal silver nanoparticles depends on the magnitude of the applied potential [4]. The shift of the LSPR position towards longer wavelengths with the increase of the potential applied to gold nanoparticles covered with a monolayer of alkanethiol was recorded in works [5,6]. These results contributed to the further development and improvement of approaches to the implementation of the ELSPR technique and its application in various fields.

In particular, ELSPR sensors have significant potential for conducting quick and inexpensive studies of various molecular processes, as well as for the sensitive detection of various biomolecular analytes. Thus, reliable and effective detection of protein phosphorylation using a combination of a field-effect device with a nanoplasmonic sensor allowed for rapid identification of novel protein kinase inhibitors [7]. A hybrid structure made of a nanopore array in a gold film and gold nanoparticles was used as an ELSPR sensor for detecting the neurotransmitters dopamine and serotonin [8]. A nanodevice based on a nanocone array decorated with silver and gold nanoparticles was used for the detection of sialic acid with a detection limit of 17 μM using electro-optical spectroscopy [9].

Various approaches have also been developed for the fabrication [10,11] and signal enhancement [12–14] of electrochemical biosensors and immunosensors using plasmonic nanostructures. For example, the combination of gold nanoparticles with carbon nanotubes and conductive polymer has led to the creation of a nanocomposite, based on which a highly sensitive impedimetric immunosensor was developed for the detection of the herbicide 2,4-dichlorophenoxyacetic acid with a detection limit of 0.3 ppb [15]. An integrated voltammetric system based on a smartphone with a sensing element coated with reduced graphene oxide and gold nanoparticles was also developed for the detection of ascorbic acid, dopamine, and uric acid in biological samples [16].

The most common approaches to implementing the regulation of LSPR through the application of an electric signal include the creation of hybrid nanomaterials such as “plasmonic nanostructure-electroactive polymer” [17–21] and “plasmonic nanostructure in a solid porous matrix” [22], as well as “liquid mirrors” [23]. It has been shown that a reversible modulation of LSPR with an amplitude of 25–30 nm is possible when an electric potential is applied to the “gold nanorod-electrochromic polymer based on a dioxythiophene derivative” system, which causes the oxidation and reduction of the polymer [17]. It has been established that the main prerequisite for significant modulation is the close overlap of the spectrum of the refractive index change of the polymer under the applied potential and the LSPR band of the nanoparticles. Similar approaches have also been implemented in the “gold nanocube-polyaniline” system for the reversible tuning of LSPR with an amplitude of up to 24 nm [18] and in the “spherical gold nanoparticle-poly(3,4-ethylenedioxythiophene)” system for observing reversible redox processes in the polymer by registering scattered light at the individual nanoparticle scale [19]. The work [20] describes an electrically-modulated plasmonic switch based on surface-enhanced Raman spectroscopy, which uses the LSPR shift under the influence of an applied electric potential to control the intensity of the Raman signal. Active plasmonic electrochromic nano-pixels of record-small area based on gold nanoparticles covered with polyaniline and located on a gold mirror provide intense colors in scattered light with electrical regulation over more than 100 nm range of wavelengths at ultra-low energy consumption, high refresh rate, and contrast [21], which is promising for the development of modern displays.

Experiments measuring the spectra of electrowetting have shown that an array of gold nanorods in an anodized aluminum oxide matrix also demonstrates the ability for electroswitching of the LSPR [22]. A reversible electrically regulated liquid mirror based on a voltage-controlled self-assembly of 16 nm plasmonic nanoparticles at the interface of two immiscible electrolytes allows switching the transparency and adjusting the spectral position of the absorption band by changing the voltage in the range of ±0.5 V [23].

The use of the ELSPR method to create so-called electro-plasmonic nanoantennas has enabled the development of non-fluorescent optical probes for ultra-sensitive recording of electrophysiological signals [24]. Electro-plasmonic nanoantennas with an optical cross-section of ~10^4 nm^2 provide reliable recording of the dynamics of electrogenic activity in cardiomyocytes with a signal-to-noise ratio of ~60–200 at kilohertz frequencies when using low-intensity light (11 mW/mm^2).

Other prospects for the application of the ELSPR technique are related to the response tuning of plasmon-enhanced sensors and novel electrochemical techniques. An LSPR modulation through the application of an electric signal enables the combination of optical and electrochemical methods for the improved control and response amplification in a number of sensing methods, which include plasmon-enhanced fluorescence [25,26] and surface-enhanced Raman spectroscopy [20,27], as well as for developing plasmon-enhanced nanoelectrocatalysts [28] and performing single-nanoparticle electrochemistry [29].

An attractive idea for the ELSPR sensing is also the use of applied electric potential to manipulate the properties of adsorption and interaction of molecules bearing electric charges of different signs and magnitudes. It is important to keep in mind that the processes affecting the ELSPR sensor response to molecular analytes under applied electric potential occur in the nanoscale region at the metal-liquid interface and require careful consideration to ensure the accuracy of ELSPR measurements. In particular, there arises the problem of correctly interpreting the obtained results, taking into account the influence of potential difference on both the object of study and the sensitive part of the sensor. Therefore, mathematical modeling of the LSPR properties of plasmonic nanostructures under applied electric potential is important.

The presented theoretical review includes the results of computer modeling of the influence of the parameters of the "gold nanoparticle-electrolyte" system on the extinction spectra and the LSPR position of the nanoparticle when applying an electric potential difference between the nanoparticle and the surrounding electrolyte, using a model based on the Mie scattering theory for spherical particles and the Stern model of the electrical double layer (EDL).

2. Features of the Optical Response of a Sensor Based on Electrochemical Localized Surface Plasmon Resonance

2.1. Description of the Developed Computer Model

Based on the theoretical description of the LSPR method presented in [30] and the gold-electrolyte interface optical properties model from [31], a computer model was developed for the simulation and analysis of the light extinction spectra for the "gold nanoparticle-electrolyte" system when an electric potential difference is applied between the nanoparticle and the surrounding electrolyte. The extinction spectra were calculated according to the Mie scattering theory for spherical particles, taking into account the excitation of multipole LSPR modes and the size effect on the dielectric function of gold:

$$\sigma_{ext} = \frac{2\pi}{\left|\vec{k}\right|^2} \sum_{l=1}^{L} (2l+1)\,\mathrm{Re}(a_l + b_l), \tag{1}$$

where σ_{ext} is the extinction cross-section, $\vec{k}$ is the wave vector of light in the surrounding medium, L is the number of accounted multipole modes, and a_l, b_l are the Mie coefficients of the scattered field. The influence of the applied electric potential on the extinction spectra was taken into account within the framework of the EDL theory by Stern. In particular, it was assumed that there are no electrochemical reactions in the system, no current flows through the interface "gold nanoparticle-electrolyte", and the EDL at the boundary behaves like a capacitor with a capacitance dependent on the value of the applied potential:

$$\frac{1}{C_{EDL}} = \frac{d_D}{\varepsilon\varepsilon_0} + \frac{1}{(2\varepsilon_{el}\varepsilon_0 z^2 e_0^2 N_A \cdot 1000c/kT)^{1/2} \cosh(ze_0U/2kT)}, \tag{2}$$

$$U_0 = U + \sqrt{\frac{8kT \cdot 1000 N_A c}{\varepsilon_{el}\varepsilon_0}} \sinh\left(\frac{ze_0U}{2kT}\right) \cdot d_D, \tag{3}$$

where ε_0 is the dielectric permittivity of vacuum, e_0 is the charge of the electron, N_A is the Avogadro constant, k is the Boltzmann constant, and the rest of the parameters are described below. The change in the magnitude of the applied potential caused the emergence of charge on the surface of the gold nanoparticle:

$$\Delta\sigma = \int_{U_{pzc}}^{U_0} C_{EDL}\, dU, \tag{4}$$

which led to a change in the concentration of free electrons in a surface layer of gold d about 1 Å thick (the penetration depth of a static electric field into the metal bulk):

$$\Delta N = \frac{\Delta\sigma}{d \cdot e_0}, \tag{5}$$

and therefore, to the corresponding change in the dielectric function of gold in this layer:

$$\Delta\varepsilon_m = (1 - \varepsilon_m^f)\frac{\Delta N}{N}, \tag{6}$$

where ε_m^f is the contribution of free electrons to the relative dielectric permittivity of the metal, N is the concentration of free electrons in the metal. The optical constants of bulk gold were taken from tables [32] and approximated using 9th-order polynomials with a wavelength step of 1 nm. To accurately determine the positions of the maxima of the simulated extinction spectra by wavelength (i.e., the position of the local maxima), a parabolic approximation around the position of the absolute maximum of the spectrum was used. The following basic parameters of the system were employed in the modeling:

- range of light wavelengths: λ = 450–700 nm;
- size of gold nanoparticles: radius a = 5, 20, 40, 60, 80 nm;
- relaxation time of electrons for bulk gold: $\tau_{bulk} = 9.3 \cdot 10^{-15}$ s [33];
- Fermi speed of electrons for gold: $V_F = 1.4 \cdot 10^6$ m/s [34];
- plasma frequency for bulk gold: $\omega_p = 1.37 \cdot 10^{16}$ rad/s [35];
- range of applied potential difference between the gold nanoparticle and the surrounding electrolyte solution: U_0 = −0.3–+0.6 V (which corresponds to the experimentally determined range of voltages, where electrochemical reactions involving sensor component materials are absent) [31];
- refractive index of the electrolyte: n = 1.33;
- concentration of free electrons in gold: $N = 5.9 \cdot 10^{28}$ m^{-3} [35];
- thickness of the dense layer of EDL: d_D = 8.5 Å (calculated according to the size of the water molecule and the SO_4^{2-} anion [36]);
- relative static dielectric permeability of the electrolyte: ε_{el} = 80 [34];
- concentration of the electrolyte: c = 0.1 mol/L;
- charge of the electrolyte ion: z = 2;
- temperature of the electrolyte: T = 293 K;
- potential of zero charge of the nanoparticle in the electrolyte: U_{pzc} = 0 V.

A multi-parameter computer model was developed to study the influence of a number of electrolyte parameters on the extinction spectra of the system and the LSPR position at different values of the applied potential difference for various sizes of gold nanoparticles. While the current approach considers the applied potential mode that is relevant for linear sweep or cyclic voltammetry, it can be extended for studying dynamic modulation (e.g., AC or pulsed potentials) by varying the input potential value as needed. This model can also be extended towards predicting sensor performance for specific analytes or Faradaic processes, as well as for considering surface roughness, by employing the effective medium theory, e.g., symmetrical Bruggeman effective medium theory [30], to describe the optical constants of multi-component layers on the surface of the nanoparticle. To consider non-spherical geometries, other analytical or numerical approaches for the simulation of extinction spectra should be used, such as generalized Mie theory for particles without sharp edges [37].

2.2. Effect of the Gold Nanoparticle Size on the Response of the ELSPR Sensor

It is known that the size of the plasmonic nanostructure critically affects its optical and sensing properties [30]. Therefore, when developing a new type of plasmonic sensor, optimizing the sizes of the nanostructures is a primary step. Using the aforementioned approach, the evolution of the extinction spectra of the "gold nanoparticle-electrolyte" system was modeled by changing the applied electric potential for the gold nanoparticle radii a = 5, 20, 40, 60, 80 nm (Figure 1).

It can be observed that the increase in the nanoparticle size predictably leads to a redshift of the LSPR position from ~525 nm for a nanoparticle radius of 5 nm (Figure 1a) to ~655 nm for a nanoparticle radius of 80 nm (Figure 1e). Additionally, it is worth noting that the extinction spectra undergo a nonlinear and mostly non-monotonic shift in intensity and wavelength depending on the magnitude of the applied potential across all nanoparticle sizes in the radius range of 5–80 nm. It has also been established that the resulting LSPR position shift when changing the potential difference in the range of −0.3 to +0.6 V depends on the nanoparticle size and can reach amplitude values from 0.9 nm to 5 nm using the aforementioned basic system parameters (Figure 1f).

At the same time, the largest shift in the LSPR position is observed for the smallest nanoparticle (a = 5 nm), while the smallest shift occurs for the largest nanoparticle (a = 80 nm), which can be explained by the reduction of the contribution from the surface layer of a gold nanoparticle with a thickness of 1 Å with a potential-dependent dielectric function of gold in the overall extinction spectrum. This is in agreement with experimental results reported in the literature. For example, dodecanethiolate monolayer-protected gold clusters (5.2 nm average diameter) subjected to electronic charging by electrolysis from rest potential (−0.16 V) to +0.82 V exhibited a 9 nm (516 to 525 nm) LSPR shift [5], while 50 nm gold colloid particles immobilized on the ITO-coated glass substrate demonstrated LSPR shifts of ~2 nm and ~2.5 nm with the potential scans from −0.2 up to +0.5 V and

from −0.2 up to +0.8 V, respectively [38]. Thus, depending on the investigated system, the relationship between the magnitude of the influence of the potential difference on the subject of research and on the sensitive part of the sensor can be adjusted by changing the size of the gold nanoparticle.

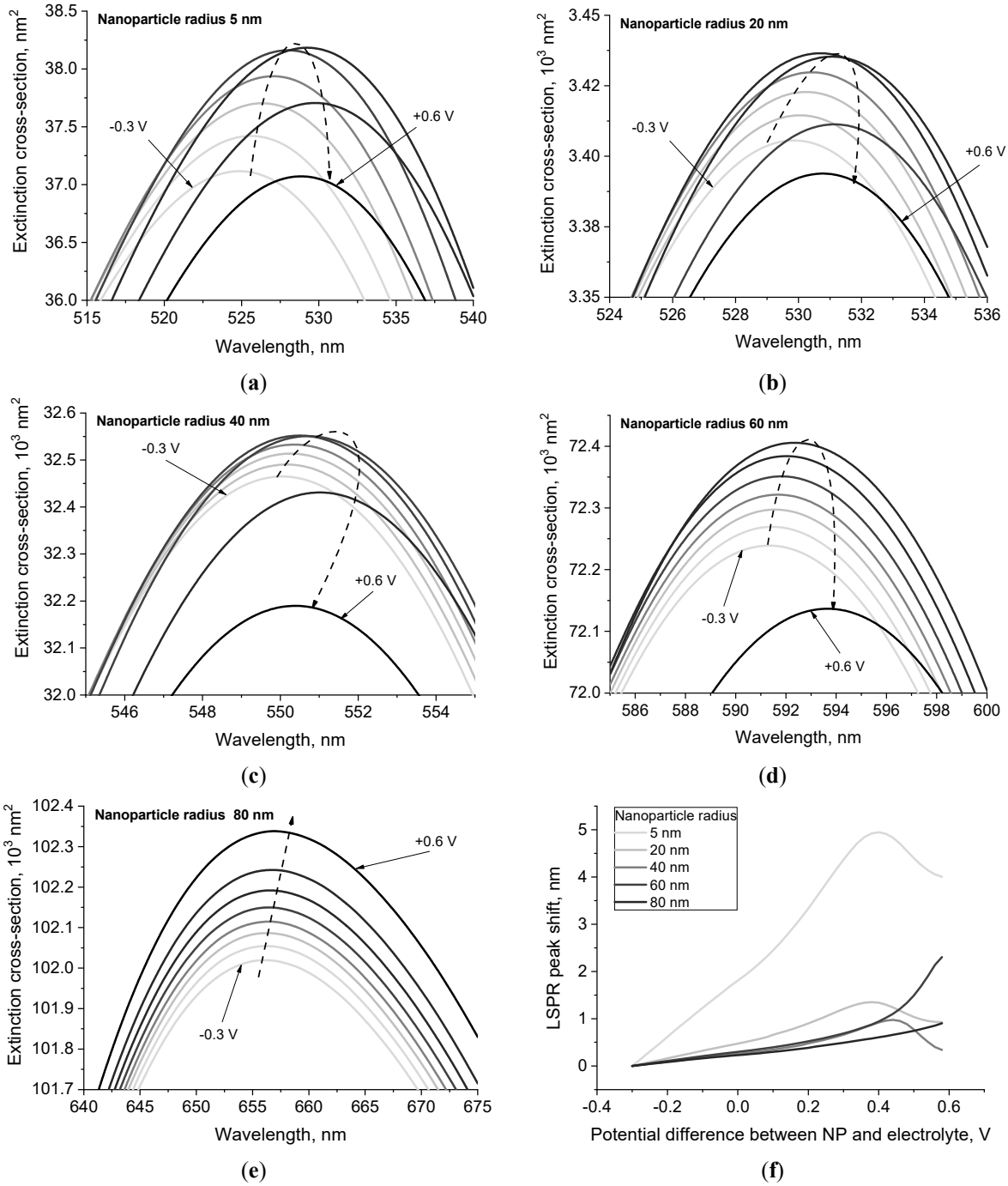

Figure 1. Simulated extinction cross-section spectra of the "gold nanoparticle-electrolyte" system with varying applied electric potential difference in the range of −0.3 to +0.6 V for the gold nanoparticle radii (**a**) 5 nm, (**b**) 20 nm, (**c**) 40 nm, (**d**) 60 nm, (**e**) 80 nm. (**f**) Dependence of the LSPR position shift on the applied electric potential difference for the gold nanoparticle radii of 5–80 nm, corresponding to spectra (**a**–**e**).

2.3. Effect of the Refractive Index of the Electrolyte on the Response of the ELSPR Sensor

The sensitivity of the optical properties of a plasmonic nanostructure to changes in the surrounding refractive index is a fundamental property used in the development of LSPR sensors [39]. Therefore, when developing a new type of plasmonic sensor, studying the effect of the medium refractive index on the sensor response and finding an accessible range of refractive index for the measurement is an important task. The medium surrounding the plasmonic nanostructures in an ELSPR sensor can be liquid aqueous and non-aqueous electrolytes, as well as solid

substances, including polymers, which have quite different refractive indices. Thus, using the aforementioned approach, the dependences of the LSPR position for the "gold nanoparticle-electrolyte" system on the applied electrical potential difference were modeled for the refractive index of the electrolyte n = 1.33–1.5 and the gold nanoparticle radii a = 5, 20, 40, 60, 80 nm (Figure 2).

From the obtained dependences, it is evident that an increase in the refractive index of the electrolyte is mainly manifested in a monotonous shift of the LSPR position dependence towards longer wavelengths (Figure 2a–e), as well as a slight shift of the peak of this dependence (if present) towards larger values of the potential difference. An exception to these observations is the radius of the gold nanoparticle equal to 80 nm, where a non-monotonic shift and transformation of the LSPR position dependence on the potential difference is observed due to the transition to the spectral dominance of the quadrupole mode of the LSPR over the dipole mode (Figure 2f). The excitation of the quadrupole mode of the LSPR is typical for large plasmonic nanoparticles, which leads, in particular, to a change in the sensitivity of the LSPR sensor [40]. This is also demonstrated in the case considered, as the shift in the LSPR position upon changing the potential difference in the range of −0.3 to +0.6 V reaches amplitude values from 0.3 to 0.9 nm for the dipole mode of the LSPR and from 1.1 to 1.2 nm for the quadrupole mode of the LSPR, which is an increase of up to 4 times (Figure 2e).

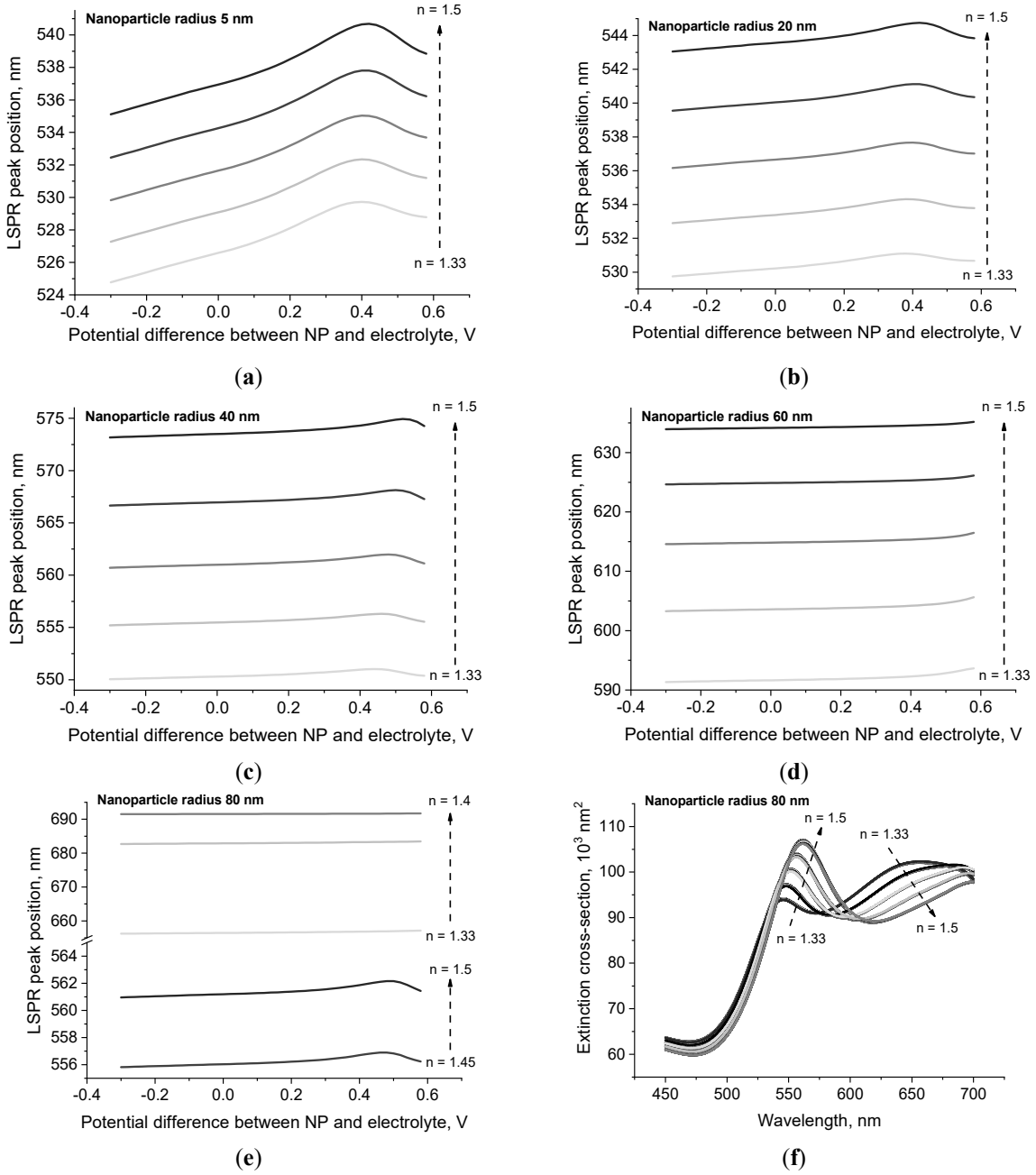

Figure 2. Modeled dependences of the LSPR position of the "gold nanoparticle-electrolyte" system on the applied electric potential difference in the range of −0.3 to +0.6 V for the refractive index of the electrolyte n = 1.33–1.5

and the radius of the gold nanoparticle of (**a**) 5 nm, (**b**) 20 nm, (**c**) 40 nm, (**d**) 60 nm, (**e**) 80 nm. (**f**) Modeled extinction cross-section spectra of the "gold nanoparticle-electrolyte" system upon changing the applied electric potential difference in the range of −0.3 to +0.6 V for the refractive index of the electrolyte n = 1.33–1.5 and the radius of the gold nanoparticle of 80 nm, which demonstrate the transition to the spectral dominance of the quadrupole mode of the LSPR over the dipole mode.

2.4. Effect of the Electrolyte Concentration on the Response of the ELSPR Sensor

According to the EDL theory by Stern, the parameters of the electrolyte affect the EDL capacitance, and thus, the optical properties of the surface layer of gold at the interface with the electrolyte. Using the approach described above, the dependences of the LSPR position for the "gold nanoparticle-electrolyte" system on the applied electric potential difference were modeled for the electrolyte concentration $c = 10^{-8}$ M–1 M and the gold nanoparticle radii a = 5, 20, 40, 60, 80 nm (Figure 3). It can be seen that the effect of increasing the electrolyte concentration is manifested in the transformation with the increase of the slope of the LSPR position dependence on the potential difference and the corresponding increase in the shift of the LSPR position per potential unit for all sizes of the gold nanoparticle.

It is worth noting the presence of a point of intersection of all dependences at a potential difference of 0 V (which corresponds to the base value of U_{pzc}), as well as a horizontal section of the dependences ranging for about 0.4 V at low electrolyte concentrations around U_{pzc}. Thus, if it is necessary to minimize the influence of the applied potential on the plasmonic nanostructure in the ELSPR sensor, for example, to study weak responses of the analyte, it is advisable to work with low electrolyte concentrations and voltages near U_{pzc}. It has also been established that the resulting shift in the LSPR position upon varying the potential difference in the range of −0.3 to +0.6 V can reach amplitudes ranging from 0.4 nm to 5.1 nm, depending on the electrolyte concentration and the size of the gold nanoparticle. This is in agreement with experimental results for 50 nm gold colloid particles immobilized on the ITO-coated glass substrate, which demonstrated LSPR shifts ranging from 0.5 to 0.8 nm after a stepwise potential was applied from 0 V to +0.25 V at electrolyte concentrations from 0.001 mM to 1000 mM, respectively [38].

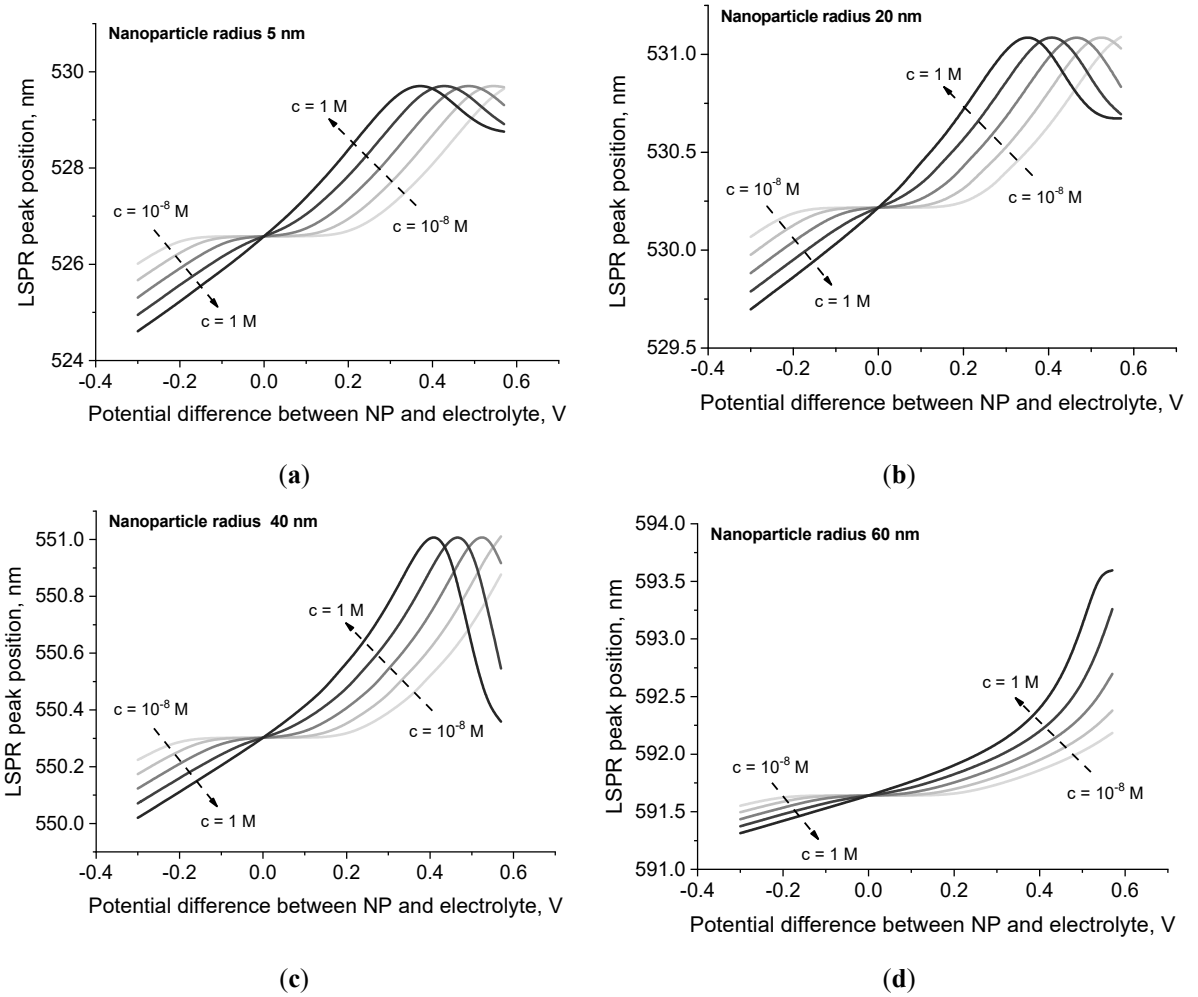

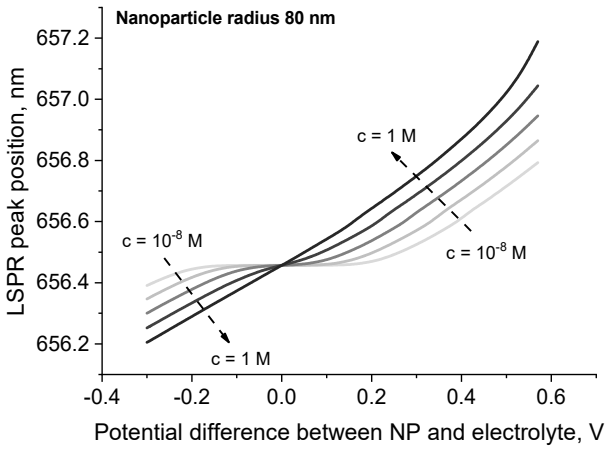

(**e**)

Figure 3. Modeled dependences of the LSPR position for the "gold nanoparticle-electrolyte" system on the applied electric potential difference in the range of −0.3 to +0.6 V for the electrolyte concentration $c = 10^{-8}$ M–1 M and the radius of the gold nanoparticle of (**a**) 5 nm, (**b**) 20 nm, (**c**) 40 nm, (**d**) 60 nm, (**e**) 80 nm.

Table 1 summarizes the resulting LSPR position shift amplitudes with changes in potential difference in the range of −0.3 to +0.6 V, depending on the size of the nanoparticle, the refractive index of the electrolyte, and the concentration of the electrolyte, which are derived from results presented in Figures 1–3 and can reach values from 0.3 nm to 5.6 nm.

Table 1. LSPR position shift amplitudes of the "gold nanoparticle-electrolyte" system upon varying applied electric potential difference in the range of −0.3 to +0.6 V, derived from Figures 1–3 for different radii of the gold nanoparticle and simulation parameter values. "D" and "Q" denote the LSPR shifts measured for dipole and quadrupole modes of the LSPR for the radius of the gold nanoparticle equal to 80 nm.

Simulation Parameter	Radius of the Gold Nanoparticle, nm				
	5	**20**	**40**	**60**	**80**
$n = 1.33$	5.0 nm	1.4 nm	1.0 nm	2.3 nm	0.9 nm (D)
$n = 1.37$	5.1 nm	1.4 nm	1.1 nm	2.3 nm	0.8 nm (D)
$n = 1.41$	5.2 nm	1.5 nm	1.3 nm	1.9 nm	0.3 nm (D)
$n = 1.45$	5.4 nm	1.6 nm	1.5 nm	1.5 nm	1.1 nm (Q)
$n = 1.49$	5.6 nm	1.7 nm	1.8 nm	1.2 nm	1.2 nm (Q)
$c = 10^{-8}$ M	3.6 nm	1.0 nm	0.7 nm	0.6 nm	0.4 nm (D)
$c = 10^{-6}$ M	4.0 nm	1.1 nm	0.8 nm	0.9 nm	0.5 nm (D)
$c = 10^{-4}$ M	4.4 nm	1.2 nm	0.9 nm	1.3 nm	0.6 nm (D)
$c = 10^{-2}$ M	4.8 nm	1.3 nm	0.9 nm	1.9 nm	0.8 nm (D)
$c = 1$ M	5.1 nm	1.4 nm	1.0 nm	2.3 nm	1.0 nm (D)

3. Conclusions

Development and recent achievements of the ELSPR methodology in the studies of molecular processes and sensitive detection of various analytes are described. Approaches for the fabrication and signal enhancement of electrochemical sensors using plasmonic nanostructures are presented. The most common and rather sophisticated configurations implementing the regulation of LSPR through the application of an electrical potential are considered, such as plasmonic nanostructures in electroactive polymers and solid porous matrices, "liquid mirrors" and electro-plasmonic nanoantennas. Prospects for the application of the ELSPR technique in response tuning of plasmon-enhanced sensors based on fluorescence and Raman scattering, as well as in novel electrochemical techniques such as plasmon-enhanced nanoelectrocatalysts and single-nanoparticle electrochemistry, are discussed.

Moreover, mathematical modeling of the LSPR properties of plasmonic nanostructures under applied electric potential is important for a deeper understanding of the processes that occur in the nanoscale region at the metal-liquid interface in ELSPR-based systems. Using a model based on the Mie scattering theory for spherical particles and the Stern theory of the electrical double layer, computer simulation was conducted to study the effect of the parameters of the "gold nanoparticle-electrolyte" system on the extinction spectra and the LSPR position of the nanoparticle upon applying an electric potential difference between the nanoparticle and the surrounding

electrolyte in the range of −0.3 to +0.6 V. A general trend has been observed towards a decrease in the shift of the LSPR position with increasing the nanoparticle size, with exceptions at certain values of other parameters. It has been demonstrated that the effect of increasing the refractive index of the electrolyte primarily manifests as a monotonic shift of the LSPR position dependence on the potential difference towards longer wavelengths, except at a radius of the gold nanoparticle of 80 nm, due to a transition to the spectral dominance of the quadrupole mode of LSPR over the dipole mode. The effect of increasing electrolyte concentration is manifested in the transformation with an increase in the slope of the LSPR position dependence on the potential difference and the corresponding increase in the aforementioned shift of the LSPR position. The developments covered in this study provide insights for future applications and the design of novel techniques based on ELSPR.

Author Contributions

A.L.: methodology, software, visualization, writing—original draft preparation; P.D.: data curation, writing—reviewing and editing; V.L.: writing—reviewing and editing; M.K.: writing—reviewing and editing; V.C.: conceptualization, supervision, writing—original draft preparation. All authors have read and agreed to the published version of the manuscript.

Funding

This work was supported by the National Research Foundation of Ukraine, project 2023.04/0057.

Data Availability Statement

Raw data of this study are available in a web repository https://github.com/lop2020/elspr.

Conflicts of Interest

The authors declare no conflict of interest. Given the role as Editorial Board Member, Volodymyr Chegel had no involvement in the peer review of this paper and had no access to information regarding its peer-review process. Full responsibility for the editorial process of this paper was delegated to another editor of the journal.

Use of AI and AI-Assisted Technologies

No AI tools were utilized for this paper.

References

1. Tadjeddine, A.; Kolb, D.M.; Kötz, R. The study of single crystal electrode surfaces by surface plasmon excitation. *Surf. Sci.* **1980**, *101*, 277–285.
2. Gordon Ii, J.G.; Ernst, S. Surface plasmons as a probe of the electrochemical interface. *Surf. Sci.* **1980**, *101*, 499–506.
3. Pettit, C.M.; Assiongbon, K.A.; Garland, J.E.; et al. Time resolved detection of electrochemical effects by surface plasmon resonance measurements: A simple technique using a large area single cell photodiode. *Sens. Actuators B Chem.* **2003**, *96*, 105–113.
4. Ung, T.; Giersig, M.; Dunstan, D.; et al. Spectroelectrochemistry of colloidal silver. *Langmuir* **1997**, *13*, 1773–1782.
5. Templeton, A.C.; Pietron, J.J.; Murray, R.W.; et al. Solvent refractive index and core charge influences on the surface plasmon absorbance of alkanethiolate monolayer-protected gold clusters. *J. Phys. Chem. B* **2000**, *104*, 564–570.
6. Riskin, M.; Basnar, B.; Chegel, V.I.; et al. Switchable surface properties through the electrochemical or biocatalytic generation of Ag^0 nanoclusters on monolayer-functionalized electrodes. *J. Am. Chem. Soc.* **2006**, *128*, 1253–1260.
7. Bhalla, N.; Di Lorenzo, M.; Pula, G.; et al. Protein phosphorylation detection using dual-mode field-effect devices and nanoplasmonic sensors. *Sci. Rep.* **2015**, *5*, 8687.
8. Li, N.; Lu, Y.; Li, S.; et al. Monitoring the electrochemical responses of neurotransmitters through localized surface plasmon resonance using nanohole array. *Biosens. Bioelectron.* **2017**, *93*, 241–249.
9. Li, S.; Liu, J.; Lu, Y.; et al. Mutual promotion of electrochemical-localized surface plasmon resonance on nanochip for sensitive sialic acid detection. *Biosens. Bioelectron.* **2018**, *117*, 32–39.
10. Putzbach, W.; Ronkainen, N.J. Immobilization techniques in the fabrication of nanomaterial-based electrochemical biosensors: A review. *Sensors* **2013**, *13*, 4811–4840.
11. Berti, F.; Turner, A.P. New Micro- and Nanotechnologies for Electrochemical Biosensor Development. In *Biosensor Nanomaterials*; Li, S., Singh, J., Banerjee, I.A., Eds.; WILEY-VCH Verlag GmbH & Co. KgaA: Weinheim, Germany, 2011.

12. Lim, S.A.; Ahmed, M.U. Electrochemical immunosensors and their recent nanomaterial-based signal amplification strategies: A review. *RSC Adv.* **2016**, *6*, 24995–25014.
13. Chikkaveeraiah, B.V.; Bhirde, A.A.; Morgan, N.Y.; et al. Electrochemical immunosensors for detection of cancer protein biomarkers. *ACS Nano* **2012**, *6*, 6546–6561.
14. Iost, R.M.; da Silva, W.C.; Madurro, J.M.; et al. Electrochemical nano(bio)sensors: Advances, diagnosis and monitoring of diseases. *Front. Biosci.* **2011**, *3*, 663–689.
15. Fusco, G.; Gallo, F.; Tortolini, C.; et al. AuNPs-functionalized PANABA-MWCNTs nanocomposite-based impedimetric immunosensor for 2,4-dichlorophenoxy acetic acid detection. *Biosens. Bioelectron.* **2017**, *93*, 52–56.
16. Ji, D.; Liu, Z.; Liu, L.; et al. Smartphone-based integrated voltammetry system for simultaneous detection of ascorbic acid, dopamine, and uric acid with graphene and gold nanoparticles modified screen-printed electrodes. *Biosens. Bioelectron.* **2018**, *119*, 55–62.
17. Ledin, P.A.; Jeon, J.W.; Geldmeier, J.A.; et al. Design of hybrid electrochromic materials with large electrical modulation of plasmonic resonances. *ACS Appl. Mater. Interfaces* **2016**, *8*, 13064–13075.
18. Jeon, J.W.; Ledin, P.A.; Geldmeier, J.A.; et al. Electrically controlled plasmonic behavior of gold nanocube@polyaniline nanostructures: Transparent plasmonic aggregates. *Chem. Mater.* **2016**, *28*, 2868–2881.
19. Zhou, J.; Panikkanvalappil, S.R.; Kang, S.; et al. Enhanced Electrochemical Dark-Field Scattering Modulation on a Single Hybrid Core–Shell Nanostructure. *J. Phys. Chem. C* **2019**, *123*, 28343–28352.
20. Zhong, L.; Jiang, Y.; Liow, C.; et al. Highly Sensitive Electro-Plasmonic Switches Based on Fivefold Stellate Polyhedral Gold Nanoparticles. *Small* **2015**, *11*, 5395–5401.
21. Peng, J.; Jeong, H.H.; Lin, Q.; et al. Scalable electrochromic nanopixels using plasmonics. *Sci. Adv.* **2019**, *5*, eaaw2205.
22. McMillan, B.G.; Berlouis, L.E.A.; Cruickshank, F.R.; et al. Reflectance and electrolyte electroreflectance from gold nanorod arrays embedded in a porous alumina matrix. *J. Electroanal. Chem.* **2007**, *599*, 177–182.
23. Montelongo, Y.; Sikdar, D.; Ma, Y.; et al. Electrotunable nanoplasmonic liquid mirror. *Nat. Mater.* **2017**, *16*, 1127–1135.
24. Habib, A.; Zhu, X.; Can, U.I.; et al. Electro-plasmonic nanoantenna: A nonfluorescent optical probe for ultrasensitive label-free detection of electrophysiological signals. *Sci. Adv.* **2019**, *5*, eaav9786.
25. Kamat, P.V.; Barazzouk, S.; Hotchandani, S. Electrochemical modulation of fluorophore emission on a nanostructured gold film. *Angew. Chem.* **2002**, *114*, 2888–2891.
26. Cameron, P.J.; Zhong, X.; Knoll, W. Electrochemically controlled surface plasmon enhanced fluorescence response of surface immobilized CdZnSe quantum dots. *J. Phys. Chem. C* **2009**, *113*, 6003–6008.
27. Lipovka, A.; Fatkullin, M.; Averkiev, A.; et al. Surface-enhanced Raman spectroscopy and electrochemistry: The ultimate chemical sensing and manipulation combination. *Crit. Rev. Anal. Chem.* **2024**, *54*, 110–134.
28. Wilson, A.J.; Mohan, V.; Jain, P.K. Mechanistic understanding of plasmon-enhanced electrochemistry. *J. Phys. Chem. C* **2019**, *123*, 29360–29369.
29. Hoener, B.S.; Kirchner, S.R.; Heiderscheit, T.S.; et al. Plasmonic sensing and control of single-nanoparticle electrochemistry. *Chem* **2018**, *4*, 1560–1585.
30. Lopatynskyi, A.M.; Lopatynska, O.G.; Guo, L.J.; et al. Localized surface plasmon resonance biosensor—Part I: Theoretical study of sensitivity—Extended Mie approach. *IEEE Sens. J.* **2010**, *11*, 361–369.
31. Lopatynskyi, A.; Guiver, M.; Chegel, V. Surface plasmon resonance biomolecular recognition nanosystem: Influence of the interfacial electrical potential. *J. Nanosci. Nanotechnol.* **2014**, *14*, 6559–6564.
32. Palik, E.D. *Handbook of Optical Constants of Solids*; Academic Press: San Diego, CA, USA 1998; 804p.
33. Johnson, P.B.; Christy, R.W. Optical constants of the noble metals. *Phys. Rev. B* **1972**, *6*, 4370.
34. Lide, R.D. *Handbook of Chemistry and Physics*, 84th ed.; CRC Press: Boca Raton, FL, USA, 2004; 2616p.
35. *Fox M. Optical Properties of Solids/M. Fox*; Oxford University Press: New York, NY, USA, 2001; 408p.
36. Bockris, J.O.; White, R.E.; Conway, B.E. *Modern Aspects of Electrochemistry*; Kluwer Academic Publishers: New York, NY, USA, 1999; 350p.
37. Papoff, F.; Hourahine, B. Geometrical Mie theory for resonances in nanoparticles of any shape. *Opt. Express* **2011**, *19*, 21432–21444.
38. Sannomiya, T.; Dermutz, H.; Hafner, C.; et al. Electrochemistry on a localized surface plasmon resonance sensor. *Langmuir* **2010**, *26*, 7619–7626.
39. Zalyubovskiy, S.J.; Bogdanova, M.; Deinega, A.; et al. Theoretical limit of localized surface plasmon resonance sensitivity to local refractive index change and its comparison to conventional surface plasmon resonance sensor. *JOSA A* **2012**, *29*, 994–1002.
40. Lopatynskyi, A.; Lopatynska, O.; Chegel, V. Comparative analysis of response modes for gold nanoparticle biosensor based on localized surface plasmon resonance. *Semicond. Phys. Quantum Electron. Optoelectron.* **2011**, *14*, 114–121.